

---

# Assessment of Infarct Size and Severity by Quantitative Myocardial SPECT: Results from a Multicenter Study Using a Cardiac Phantom

Michael K. O'Connor, Lai K. Leong, and Raymond J. Gibbons

*Departments of Radiology and Cardiology, Mayo Clinic, Rochester, Minnesota*

---

The aim of this study was to determine the reproducibility of measurements of the size and severity of myocardial defects from  $^{99m}\text{Tc}$  sestamibi cardiac phantom studies performed on multiple different gamma camera systems. **Methods:** A total of 250 gamma camera systems were evaluated over a 5-y period as part of the validation process of multiple multicenter trials. Each laboratory performed 9 acquisitions of a cardiac phantom. Small myocardial defects (0%–30% of myocardial mass) were placed in the inferobasal region, whereas larger defects (40%–70%) were located in the anterior wall. Five representative short-axis slices were analyzed to determine defect size and severity (i.e., contrast in defect region) using circumferential short-axis count profiles. Defect size and severity were analyzed as a function of the type of collimator, gamma camera system, and type of orbit (180° versus 360°). **Results:** Of the 250 systems, image data were acquired correctly and showed an acceptable correlation between true and measured defect size in 198 systems. For these systems, the slope of the regression line between true and measured defect size was  $1.03 \pm 0.03$ , with an average absolute error in estimating defect size of  $1.7\% \pm 0.5\%$  and a correlation coefficient  $r = 0.99 \pm 0.01$ . Results were independent of the gamma camera system, type of collimator, and orbit. Contrast in the defect region (minimum count/maximum count) showed a small dependence on collimator resolution and pixel size but was altered significantly by the type of acquisition orbit, with a 360° orbit showing better contrast for defects located in the inferobasal wall than a 180° orbit. **Conclusion:** Measurement of defect size is independent of the gamma camera system, type of collimator, and orbit. Contrast in small defects located in the inferobasal wall of the heart is affected significantly by the type of acquisition orbit but not by the type of collimator.

**Key Words:** SPECT; cardiac phantom;  $^{99m}\text{Tc}$  sestamibi; multicenter trials

**J Nucl Med 2000; 41:1383–1390**

---

Over the last 5–10 y, numerous tomographic techniques have been developed for the quantitative assessment of myocardium at risk and infarct size from  $^{99m}\text{Tc}$  sestamibi

myocardial perfusion studies. These techniques have used a variety of methods to assess infarct size, including polar maps (1), planimetry of the short-axis images (2), and circumferential count profile analysis of the short-axis slices (3–5). With an appropriate threshold level to discriminate infarcted from normal myocardium, all 3 methods have shown similar results (6). Furthermore, previous work from this laboratory has shown the feasibility of using these techniques for the assessment of infarct size in multicenter trials (7). In addition to the measurement of infarct size, measurement of other parameters, such as the apparent severity of the infarct, can yield useful clinical information on collateral blood flow (8,9). However, a parameter such as defect severity is in essence a measure of image contrast and, as such, is likely to be more sensitive to differences in the type of imaging equipment and the acquisition parameters.

The extension of our work to a large number of clinical sites as part of several multicenter trials has provided us with a unique opportunity to evaluate the effects of various acquisition parameters on the measurement of infarct size and the severity in a well-defined phantom model of the heart. A better understanding of the influence and importance of various acquisition parameters not only clarifies the use of quantitative information from  $^{99m}\text{Tc}$  sestamibi myocardial perfusion studies in multicenter trials but also provides important insights regarding the effect of gamma camera, collimator, acquisition orbit, and pixel size on defect size and severity.

## MATERIALS AND METHODS

### Study Group

Over a 5-y period, a total of 250 gamma camera systems were evaluated as part of the validation process for entry into 8 multicenter trials. All 8 trials were designed to assess the efficacy of various adjunctive therapies to thrombolysis and percutaneous transluminal coronary angioplasty and used measurement of infarct size as 1 of their endpoints. The validation process for myocardial perfusion imaging included several quality control tests and imaging of a cardiac phantom containing various simulated infarcts, as described (7). Of the 250 gamma camera systems, 198

---

Received May 4, 1999; revision accepted Jan. 19, 2000.  
For correspondence or reprints contact: Michael K. O'Connor, PhD, Section of Nuclear Medicine, Charlton 1-225, Mayo Clinic, Rochester, MN 55905.

successfully passed this validation process, and the cardiac phantom results from these systems are presented in this article. Fifty-two systems were excluded from this study for various technical and procedural reasons. Technical problems included nonuniformities or center-of-rotation errors with the gamma camera that degraded the image data. Procedural problems with the cardiac phantom included poor image contrast associated with the placement of incorrect activities in the myocardium and background, incorrect placement of the myocardial defects, and poor imaging technique (e.g., large collimator-to-phantom separation), which resulted in a poor correlation between true and measured defect sizes.

Of the 198 systems that passed the validation process, most (160 systems) were located in either the United States or Canada. The remaining 38 systems were located in Europe (17 systems), South America (13 systems), or Australia (8 systems). Virtually all gamma camera manufacturers were represented in this study. Table 1 presents a breakdown of the number of systems from each vendor, together with details of whether the system was a single-head, dual-head (90° orientation), or triple-head detector system.

All data were submitted by 1 of 3 methods—floppy diskette, streamer tape, or transfer using the file transfer protocol over the Internet—and either in vendor-specific file format or in Interfile (10). For the cardiac phantom data, all laboratories were asked to submit only raw planar data. Where possible, data were submitted with the appropriate uniformity and center-of-rotation corrections. Alternatively, these corrections were applied in-house using correction maps supplied by the participating laboratory. All data were

then converted to a file format compatible with the computer system used in the core laboratory (Pinnacle system; Medasys, Inc., Ann Arbor, MI).

### Quality Control

In addition to the uniformity and center-of-rotation corrections, each laboratory was required to perform several tests on system performance (7). Briefly, these tests were designed to check variation in system uniformity with rotation, collimator sensitivity and hole alignment, gantry alignment, and pixel size.

### Multicenter Cardiac Phantom Studies

The methodology for the cardiac phantom studies has been described (3,4,7). All participating laboratories were supplied with a cardiac phantom (RH-2; Capintec, Ramsey, NJ) containing a heart, lungs, and a spine. The phantom had an outside circumference of 85 cm. The heart consisted of right and left ventricles with separate compartments for the blood pool and myocardium. Eight latex insets (defects), ranging in size from 5% to 70% of myocardial volume, were used to simulate hypoperfused or infarcted myocardium. Each laboratory performed a total of 9 SPECT acquisitions with the phantom, 1 for each defect and 1 with no defect. Laboratories were requested to place the small defects (5%–30%) in the inferobasal region of the heart and the large defects (40%–70%) in the anterior wall of the heart. For the study of the normal myocardium, 74 MBq (2 mCi) <sup>99m</sup>Tc were placed in the background chamber of the phantom and 56 MBq (1.5 mCi) <sup>99m</sup>Tc were placed in the myocardium. With the introduction of various defects, myocardial activity was reduced in proportion to defect size. In a previous study we showed that these activities result in a myocardial-to-background ratio of 1.86 for a normal myocardium (3). When allowance is made for the presence of cardiac disease, this ratio is comparable with the value of 1.64 found in clinical studies (3).

Laboratories were allowed to use their standard clinical procedure for <sup>99m</sup>Tc sestamibi SPECT imaging of the heart, with the following minimum requirements. Acquisitions were to be performed in a 64 × 64 matrix and were required to contain at least 30 views over 180° or 60 views over 360° if acquired in step-and-shoot mode or twice that amount for continuous-mode acquisitions. Body contouring or elliptic orbits were permitted, providing that corrections for the noncircular nature of the orbit were applied to the submitted data. Laboratories were permitted to use their preferred collimator for <sup>99m</sup>Tc sestamibi studies and were asked to specify the type of collimator and its rated sensitivity. The use of nonparallel hole collimators was not permitted because of the difficulty in accurately reconstructing such data.

All tomographic studies were reconstructed in an identical manner. Filtered backprojection was applied using a Hann filter with a cutoff at 0.7-Nyquist frequency. From the reconstructed short-axis slices of the heart, 5 representative slices were selected using predetermined rules (3) (apical, midventricular, and basal slices and 2 intermediate slices midway: 1 midway between the apex and midventricle and the other midway between the midventricle and the base). Circumferential count profiles were generated for each of the 5 slices by identifying the peak counts every 6° around the left ventricle. The size of the perfusion defect was quantitated from these 5 slices using a previously published and well-validated technique (3,7). Briefly, defect size was determined from the fraction of radians (60 per count profile) that fell below a threshold of 60% of peak counts in each slice. From the above analysis, measured defect size was correlated with true defect size

**TABLE 1**  
Breakdown of 198 Systems by Manufacturer and Number of Detector Heads

Manufacturer	Detector system		
	Single head	Dual head	Triple head
ADAC Laboratories*	16	17	—
Elsint†	32	3	—
Mediso‡	4	—	—
General Electric Medical Systems§	39	4	—
Picker International	2	—	12
Siemens Medical Systems¶	39	—	2
Sopha/Summit Medical Systems#	14	7	—
Toshiba**	2	—	2
Trionix††	—	—	3
<b>Total</b>	<b>148</b>	<b>31</b>	<b>19</b>

\*Milpitas, CA.

†Haifa, Israel.

‡Budapest, Hungary.

§Milwaukee, WI.

||Cleveland Heights, OH.

¶Hoffman Estates, IL.

#Buc, France.

\*\*Tokyo, Japan.

††Twinsburg, OH.

Dual-detector systems with opposing (unused) detector have been classified as single-detector systems.

by linear regression analysis. The slope and intercept of the regression line were determined. The absolute error between the true and measured defect size was determined for each of the 9 studies, and the average value of this error (average absolute error) was determined for each system.

The severity of the defects (i.e., defect contrast) was calculated from the ratio of the minimum to maximum counts in each of the 5 slices, with the lowest value (nadir) being recorded (11). In theory, the nadir should have a value of 1 for a normal myocardial study and a value of 0 for studies with defects present. From the normal myocardial study, the mean value of the circumferential count profile for each of the 5 slices was obtained and normalized to the mean value of the apical slice.

All the above results were categorized as a function of several variables. These variables included the manufacturer, the number of detector heads, the type of acquisition orbit (180° versus 360°), the type of collimator, and the pixel size.

### In-House Cardiac Phantom Studies

Although data from a large number of systems were collected as part of this study, variability in how studies were performed and the limited amount of data acquired under certain conditions made it difficult to ascertain the influence of some acquisition parameters. Hence, to confirm some findings from the multicenter data we performed a series of cardiac phantom studies on a dual-head (opposing detectors) Helix system (Elscent Ltd., Haifa, Israel). The methodology for the cardiac phantom studies was identical to that described above with the following modifications. Each defect was imaged twice, once positioned in the inferior wall and once positioned in the anterior wall. All studies were performed using a 360° orbit, and both 360° and 180° reconstructions were performed. Replicate studies were performed using low-energy, general-purpose (LEGP) and low-energy, high-resolution (LEHR) collimators. Sensitivity was measured at 6.76 counts/min/kBq (250 counts/min/ $\mu$ Ci) and 4.05 counts/min/kBq (150 counts/min/ $\mu$ Ci) for the LEGP and LEHR collimators, respectively. Collimator resolution was measured at 7.8 and 6.9 mm at 10 cm in air for the LEGP and LEHR collimators, respectively. All data reconstruction and analysis were performed as described.

### Statistical Analysis

The significance of differences in values of the slope of the regression line relating true versus measured defect size and

average absolute error in estimating defect size for single-, dual-, and triple-head gamma camera systems were determined by 1-way ANOVA. One-way ANOVA was also used to determine the significance of acquisition orbit and collimation on the average counts in each of the 5 short-axis slices from apex to base of the heart. For the multicenter data, comparisons of the effects of pixel size and collimator resolution on defect severity were performed using a paired *t* test. A paired *t* test analysis was also used for comparison of the effect of acquisition orbit; however, the analysis was limited to small defect sizes (5%–30%). No statistical analysis was performed on the in-house studies because these data contained only a single measurement at each defect size.

## RESULTS

Approximately 75% (148 systems) of systems in this study were single-head systems. This percentage includes opposing dual-head systems in which the second detector was not used. There were 31 90° dual-head systems and 19 triple-head systems.

The slope of the regression line relating true versus measured defect size (Fig. 1A) and the absolute error in estimating infarct size (Fig. 1B) are plotted as a function of the number of detector heads. Using 1-way ANOVA, the mean value of the slope was found to be similar for single- and dual-head systems ( $1.03 \pm 0.03$ ) but was significantly different ( $P = 0.001$ ) for triple-head systems ( $1.00 \pm 0.02$ ). The average absolute error in estimating defect size was  $1.69\% \pm 0.52\%$  for single-head systems,  $1.58\% \pm 0.52\%$  for dual-head systems, and  $1.47\% \pm 0.53\%$  for triple-head systems. These differences were not significant. The most notable difference in how data were acquired between the triple-head systems and the single- or dual-head systems was the type of acquisition orbit. All studies were acquired with a 360° orbit on triple-head systems and a 180° orbit on single- or dual-head systems.

To determine the effects of collimator resolution on the quality of the cardiac phantom studies, we used collimator sensitivity as an indicator of resolution. Because of the variety and vintage of systems studied, there was consider-

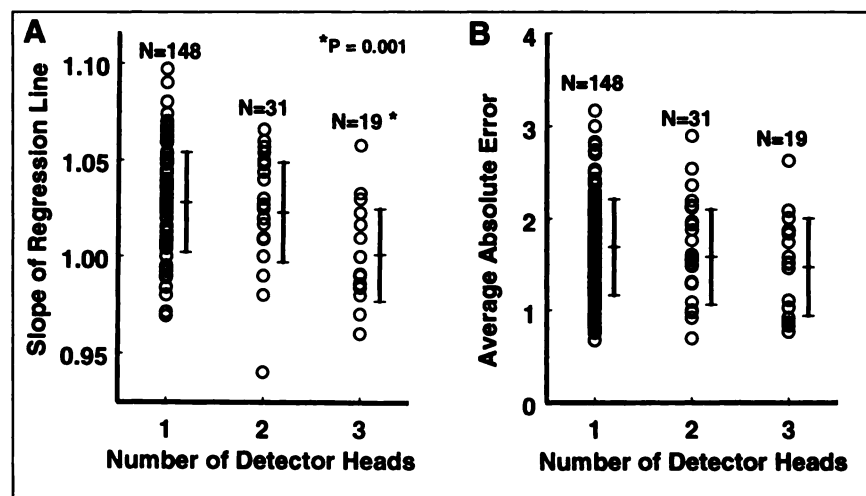


**FIGURE 1.** Scattergram showing values for slope of regression line (correlating true vs. measured defect size) (A) and average absolute error in estimating defect size (B) for 198 systems. Results are plotted for single-head, dual-head (90°), and triple-head systems. Values of average absolute error were not significantly different between systems; however, values of slope of triple-head systems were significantly different from those of single- or dual-head systems ( $P = 0.001$ ).

able variation in how collimators were classified. In addition, the measured sensitivity of a collimator often varied substantially for a given rated sensitivity (Fig. 2). For the purposes of this study, we arbitrarily classified collimators with a rated sensitivity of  $>8.11$  counts/min/kBq (300 counts/min/ $\mu$ Ci) as low resolution (LEGP) and those with a rated sensitivity of  $<5.41$  counts/min/kBq (200 counts/min/ $\mu$ Ci) as high resolution (LEHR). Systems with an intermediate collimator sensitivity ( $>5.41$  but  $<8.11$  counts/min/kBq [ $>200$  but  $<300$  counts/min/ $\mu$ Ci]) were excluded from this analysis. This resulted in the elimination of 66 systems from the analysis.

An additional parameter that was considered in comparing systems was pixel size. A very large pixel size would be expected to reduce the accuracy of any measurement of defect size or severity. Figure 3 plots the range of pixel sizes observed in all systems as a function of the number of detector heads. An arbitrary cutoff of 0.7 cm/pixel was chosen to classify studies as having been acquired with a small or large pixel size.

Figure 4A plots the effect of pixel size on the value of the nadir for the normal myocardium and the 8 studies containing defects. Results have been limited to the 75 systems performing a  $180^\circ$  acquisition orbit (single- or dual-head systems) and equipped with a high-resolution collimator as defined. Seven of these systems had a pixel size of  $\geq 7$  mm. Paired *t* test analysis showed a small but significant loss in image contrast with the larger pixel size ( $P = 0.002$ ) for all 8 defects. For systems performing a  $360^\circ$  orbit, no effect of pixel size could be shown, possibly because of the limited number of systems available for comparison and the absence

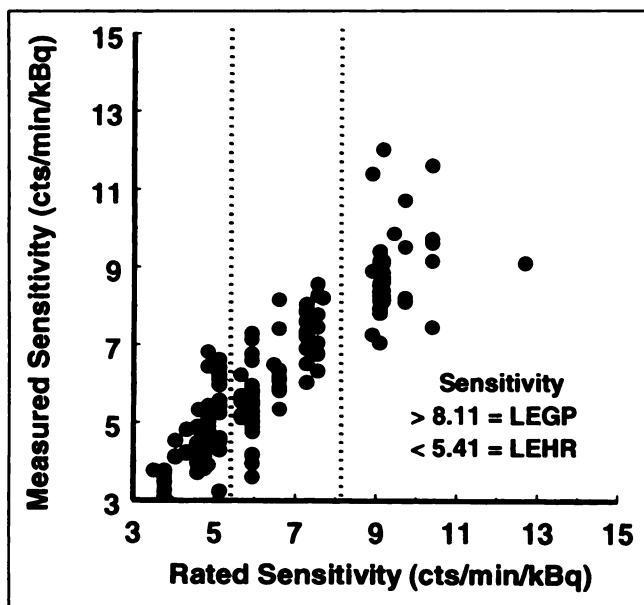


**FIGURE 2.** Relationship between rated (by manufacturer) and measured collimator sensitivity for 198 systems. Collimators with rated sensitivities of  $>8.11$  counts/min/kBq (300 counts/min/ $\mu$ Ci) were classified as all purpose (LEGP) and  $<5.41$  counts/min/kBq (200 counts/min/ $\mu$ Ci) as high resolution (LEHR).

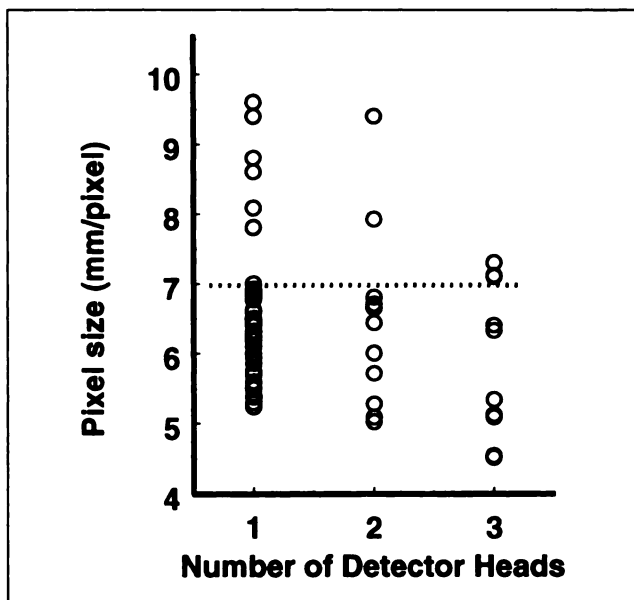


**FIGURE 3.** Scattergram showing measured pixel sizes for 198 systems. Large pixel size was arbitrarily defined as  $>7$  mm/pixel. Results are plotted for single-head, dual-head ( $90^\circ$ ), and triple-head systems.

of any systems with a pixel size substantially greater than 7 mm (Fig. 3). Figure 4B plots the effect of collimator resolution on the value of the nadir. The mean sensitivities for collimators defined as LEHR and LEGP were  $4.54 \pm 0.49$  counts/min/kBq ( $168 \pm 18$  counts/min/ $\mu$ Ci) and  $9.30 \pm 0.70$  counts/min/kBq ( $344 \pm 26$  counts/min/ $\mu$ Ci), respectively. Results have been limited to the 111 systems performing a  $180^\circ$  acquisition orbit (single- or dual-head systems) and having a pixel size of  $<7$  mm/pixel. As with pixel size, paired *t* test analysis showed that improved resolution leads to a small but significant improvement in image contrast ( $P < 0.001$ ) for the 8 defects. Figure 4C plots the effect of the type of acquisition orbit ( $180^\circ$  versus  $360^\circ$ ) on the value of the nadir for the normal myocardium and the 8 studies containing defects. Results have been limited to the 81 systems equipped with a LEHR collimator and a pixel size of  $<7$  mm/pixel. Paired *t* test analysis showed that data acquired with a  $360^\circ$  orbit resulted in significant gains in image contrast for defects located in the inferobasal wall of the heart ( $P < 0.0001$  for 5%–30% defects). No significant difference in image contrast was seen for the larger defects (40%–70% defects) located in the anterior wall of the heart ( $P =$  not significant). No meaningful comparison was possible between the LEHR and LEGP collimators on systems performing a  $360^\circ$  orbit because only 1 of the triple-head systems evaluated in this study used LEGP collimators.

Figure 5 plots the mean counts from apex to base in the 5 short-axis slices from the normal myocardial study. Results are shown as a function of type of orbit and collimator resolution and are normalized to the average counts in the apical slices. Using 1-way ANOVA for each short-axis slice,

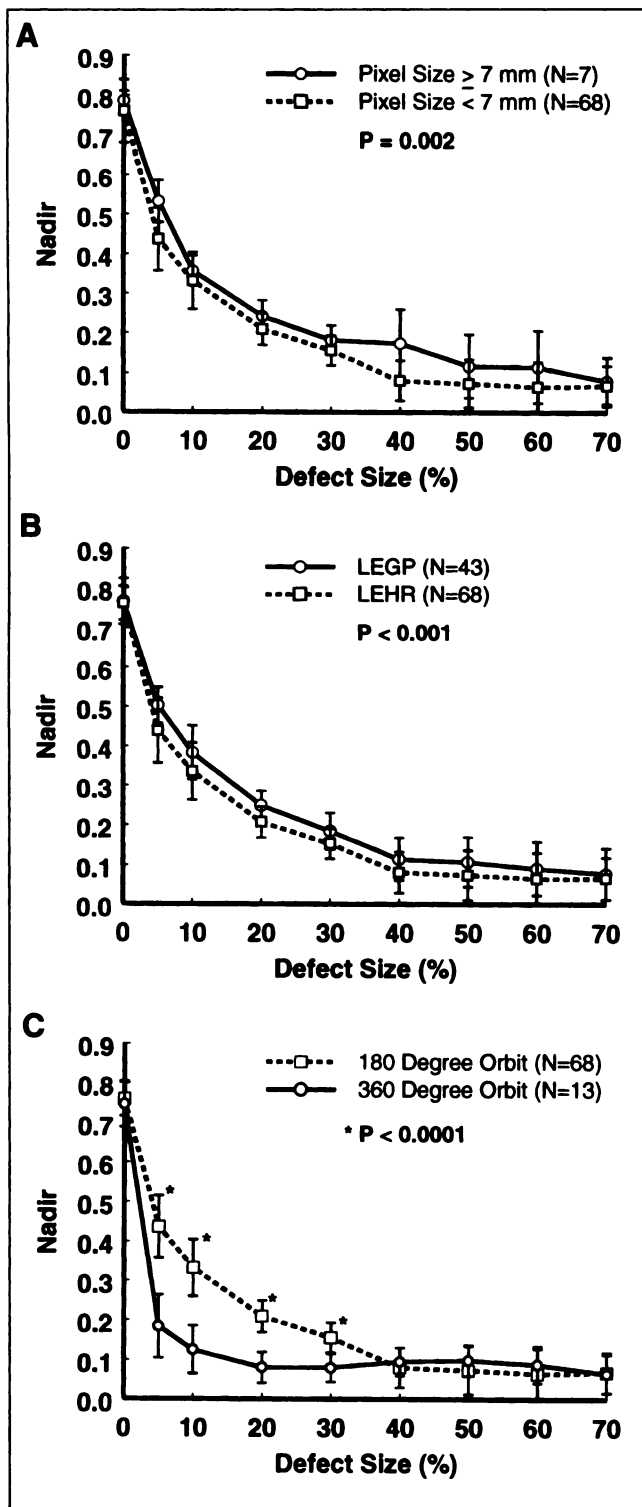


**FIGURE 4.** (A) Relationship between defect nadir and defect size as function of pixel size. Results are limited to systems equipped with high-resolution collimators and performing 180° acquisition orbit (n = 75). (B) Relationship between defect nadir and defect size as function of type of collimator. Results are limited to systems with pixel size  $< 7$  mm and performing 180° acquisition orbit (n = 111). (C) Relationship between defect nadir and defect size as function of type of acquisition orbit. Results are limited to systems with pixel size  $< 7$  mm and equipped with high-resolution collimator (n = 81). \*Paired *t* test gave significant *P* only for defect sizes 5%–30%.

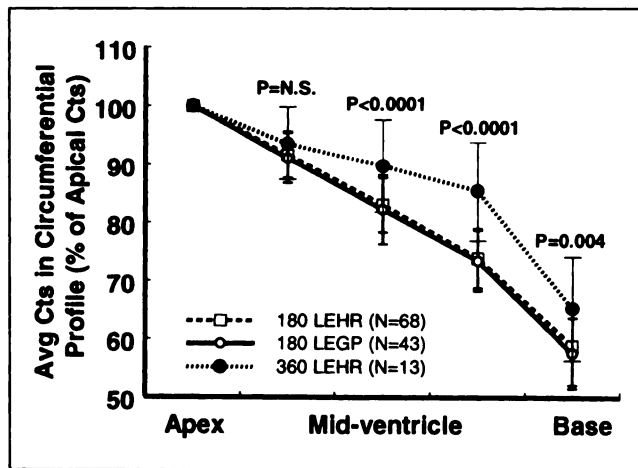


**FIGURE 5.** Mean counts in circumferential count profile for 5 selected short-axis slices from normal myocardium. Results are shown as function of acquisition orbit and collimator type and are normalized to average counts in apical slice. *P* was significant only for orbit (180° vs. 360°). N.S. = not significant.

no significant effect of collimator resolution was found; however, data acquired with a 360° orbit showed better uniformity of counts from apex to base, which was significant ( $P \leq 0.004$ ) for results from the midventricle to base.

Results from all systems were also evaluated as a function of the vendor. No significant difference was found in image contrast as a function of the system vendor, even after allowing for differences in collimator sensitivity, pixel size, and acquisition arc. This may be associated with the large variety of systems of different vintages within a given manufacturer. One noticeable exception to the above was the difference in image quality between data acquired on Picker triple-head systems (Picker International, Inc., Cleveland Heights, OH) and other vendors' systems. This difference was thought to be associated with the acquisition orbit rather than with the vendor. In-house studies were performed to confirm this fact.

The results of in-house cardiac phantom studies concur with those from the multicenter data. Figure 6A compares the effect of acquisition orbit and defect location on image contrast. The results agree with those shown in Figure 4C for defects placed in the inferior or inferobasal wall. When defects were placed in the anterior wall, there was no significant difference in image contrast as a function of orbit except for the smallest defect, where even in the anterior position the 360° orbit appears to offer slightly improved contrast over a 180° orbit. Figure 6B examines the effect of collimator resolution and type of orbit. The results confirm the findings shown in Figure 4B and indicate an improvement in image contrast with a LEHR collimator versus a LEGP collimator irrespective of the type of acquisition orbit.

## DISCUSSION

Large-scale multicenter studies incorporating the use of SPECT, as described in this article, have not been performed

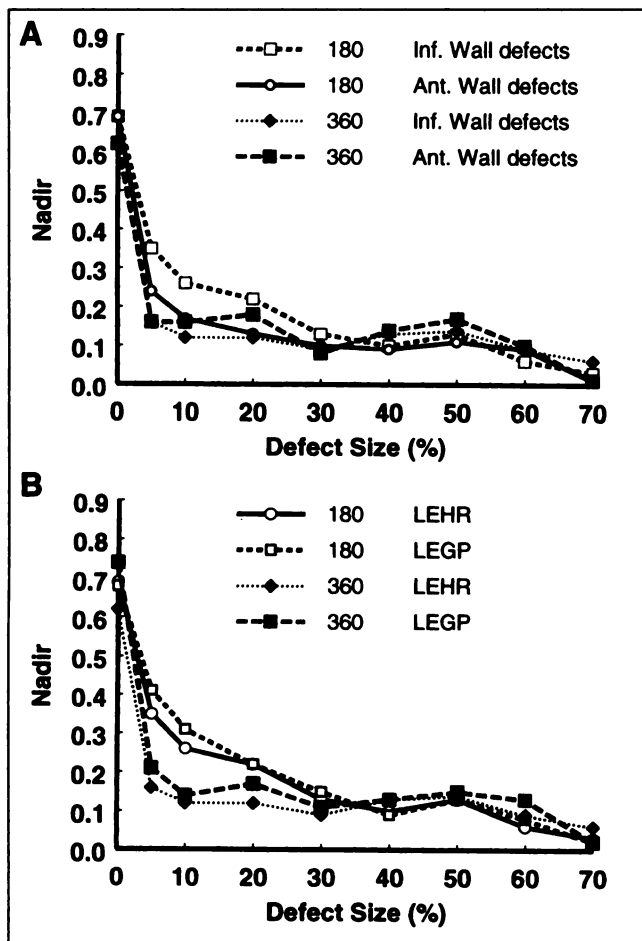


**FIGURE 6.** (A) Results from in-house study showing relationship between defect nadir and defect size as function of acquisition orbit and defect location in myocardium. System was equipped with high-resolution collimators and had pixel size of 5.9 mm/pixel. Inf. = inferior; Ant. = anterior. (B) Results from in-house study showing relationship between defect nadir and defect size as function of acquisition orbit and type of collimator. Defects were located in inferior or inferoseptal walls of heart. Pixel size was 5.9 mm/pixel.

previously because of the high cost and logistical difficulties involved. Our results represent the cumulative data of 8 large multicenter trials. They provide a unique opportunity to evaluate many of the technical aspects of myocardial perfusion imaging independently of the specific performance characteristics of a given manufacturer's gamma camera system.

Our previous pilot study of 22 systems showed the feasibility of SPECT myocardial perfusion imaging in a multicenter trial setting (7). The purpose of this study was to clarify the effects of many system-dependent acquisition parameters on the measurement of defect size and severity. The purpose of the in-house studies was 2-fold. First, it allowed us to confirm the findings of our multicenter data and confirmed that the results shown in Figures 4B and C were related to type of collimator and acquisition orbit and were not the result of some unique feature on a specific

vendor's gamma camera. This was particularly important in the issue of 180° versus 360° because most systems performing 360° orbits were manufactured by 1 vendor. Second, the in-house studies allowed us to examine the influence of defect location on defect contrast. This was not practical in the multicenter studies because of the time-consuming nature of the validation process.

This study confirms the findings of our previous pilot study and indicates that the results obtained from measurement of infarct size are relatively uniform and consistent across many different tomographic systems. Although we have used our own technique for measurement of infarct size, an independent study (6) has shown that equivalent results can be obtained with the techniques of Verani et al. (1) and Tamaki et al. (2). This confirmation indicates that quantitative estimation of infarct size is possible and relatively invariant between many different types of imaging systems and analytic techniques. For the particular phantom model used in this study, the accuracy with which a particular system can measure infarct size appears to be better for systems performing a 360° orbit than those performing a 180° orbit. This issue is discussed in more detail below.

During myocardial infarction, the residual activity in the infarct region as measured by the nadir has been shown to correlate with collateral blood flow to that region (11). Figures 4-6 show that measurement of the nadir is influenced by a large number of variables: pixel size, collimator resolution, type of orbit, and defect size and location within the heart. These variables are in addition to reconstruction software and filtration, which were controlled in this study. Our previous pilot study showed that these 2 reconstruction variables influenced measurement of infarct size (7). We believe that they also influence image contrast (7). Therefore, in a multicenter study attempting to use image contrast as an endpoint, tight control over all aspects of image acquisition and analysis is required for meaningful comparison of data.

At present, most (69%) laboratories in the United States perform <sup>99m</sup>Tc myocardial perfusion studies using high-resolution or ultra-high-resolution collimators (12). Whereas a higher resolution collimator will undoubtedly yield a higher resolution image, it is not certain that this gain translates into an improvement in sensitivity for the detection of disease. Figures 4B and 6A indicate only a small improvement in image contrast with a high-resolution collimator. This small gain needs to be balanced against the loss in sensitivity (a factor of 2) with a high-resolution collimator. Any increase in patient motion that results from the longer acquisition is likely to offset the gains in image contrast. This study did not include any gated SPECT studies. By eliminating the blurring effects of wall motion, it is possible that gating may enhance the differences in collimator resolution.

Although the benefits of high-resolution versus all-purpose collimation can be debated, the adverse effects of a

large pixel size are unequivocal. Figure 4A shows that the minor benefit in image contrast achieved with a high-resolution collimator (Fig. 4B) is essentially eliminated if the pixel size is too large. In this study, approximately 10% of laboratories used a pixel size >7 mm. In all cases, this occurred on large field-of-view systems (>50 cm) with no zoom. This may reflect a failure to account for the increased pixel size that occurs when an old standard 40-cm field-of-view system is replaced by a modern 50- to 55-cm field-of-view system. The effect of pixel size may have been further exacerbated by the use of a standard cutoff frequency (0.7 Nyquist) in the image reconstruction that will result in greater smoothing of images acquired with a larger pixel size.

Surprisingly, the parameter that appears to have the greatest impact on image contrast is the type of orbit. The issue of 180° versus 360° has been discussed in the literature since the early 1980s (13–15). Whereas a 180° acquisition orbit provides superior image contrast for anterior and anterolateral wall defects in perfusion studies with <sup>201</sup>Tl, several studies have shown that this improved contrast comes at the expense of significant image distortion (16,17). Although a 1982 editorial suggested that “the probable introduction of new myocardial imaging agents using <sup>99m</sup>Tc. . . will (eventually) outweigh the advantages of the 180° sweep” (18), few studies have critically examined the significance of the type of orbit on the detection of perfusion defects in different parts of the heart using <sup>99m</sup>Tc perfusion agents. Limited patient and phantom studies by Maublant et al. (19) and Folks et al. (20) concluded that there did not appear to be any advantage of a 360° orbit over a 180° orbit. In the absence of a compelling reason to alter clinical practice, a 180° acquisition orbit has remained the standard for cardiac SPECT imaging with <sup>99m</sup>Tc.

The data from this multicenter study suggest that for certain types of defects—in particular, small defects in the inferior wall—a 360° orbit may yield significantly better contrast than a 180° orbit. The in-house studies confirm this and also show some advantage of the 360° orbit for the small (5%) anterobasal wall defect (Fig. 6A). For quantitative analysis of defect severity, the type of orbit may play a more critical role than other parameters such as collimation, particularly for small defects located near the base of the heart. Although the cardiac phantom used in this study is representative of a normal human chest, it is unlikely to adequately reflect results that may be obtained in the large or obese patient. Such patients represent a significant percentage of the patient population seen in nuclear cardiology laboratories in the United States (21). Clarification of the 180° versus 360° issue for cardiac imaging will require a study that evaluates image contrast in different regions of the heart in a representative spectrum of patients. Despite the widespread clinical use of <sup>99m</sup>Tc-based myocardial imaging agents for more than 5 y, such a study has not yet been performed. This issue will become more important as efforts proceed to reduce artifacts caused by soft-tissue attenuation,

the presence of adjacent hot liver or bowel activity, and patient motion. With filtered backprojection, such artifacts are far more severe with a 180° acquisition compared with a 360° acquisition (22). Recent work with maximum likelihood algorithms suggests that the use of these algorithms together with attenuation correction may minimize the effect of the acquisition orbit on image quality (22,23).

The primary limitations of this study center on the dimensions of the cardiac phantom. With an outside circumference of 85 cm, the cardiac phantom is similar to that of a small adult and is not representative of the population seen in our laboratory, where average chest circumference is approximately 110 cm (24). It is possible that with increasing chest circumference, the advantages or disadvantages of specific acquisition orbits and the effects of collimator resolution may be altered substantially.

## CONCLUSION

In this large multicenter study we found that measurement of defect size was essentially independent of the type of gamma camera, acquisition orbit, and collimator. However, contrast in the defect region was strongly influenced by the acquisition orbit and to a lesser degree by the type of collimator and pixel size. These results suggest that the issue of the optimal acquisition orbit for cardiac SPECT imaging should be reassessed.

## ACKNOWLEDGMENTS

The authors appreciate the considerable amount of work undertaken by all laboratories that participated in the multicenter trials and also thank Chip Jordan and Mona Hopfenspirger for their work in data processing and management of the phantoms. Financial support for this work was obtained in part from Burroughs-Wellcome Laboratories, Cytel Ltd., Genentech Ltd., ICOS Ltd., Medco Ltd., and Rhone-Poulenc-Rorer Ltd. This work was presented in part at the 45th Annual Meeting of the Society of Nuclear Medicine, Toronto, Ontario, Canada, June 7–11, 1998.

## REFERENCES

1. Verani MS, Jeroudi MO, Mahamarian JJ, et al. Quantification of myocardial infarction during coronary occlusion and myocardial salvage after reperfusion using cardiac imaging with technetium-99m hexakis 2-methoxyisobutyl isonitrile. *J Am Coll Cardiol*. 1988;12:1573–1581.
2. Tamaki S, Nakajima H, Murakami T, et al. Estimation of infarct size by myocardial emission computed tomography with thallium 201 and its relation to creatine kinase-MB release after myocardial infarction in man. *Circulation*. 1982;66:994–1001.
3. O'Connor MK, Hammell T, Gibbons RJ. In vitro validation of a simple tomographic technique for estimation of percent myocardium at risk using methoxyisobutyl isonitrile technetium-99m (sestamibi). *Eur J Nucl Med*. 1990;17:69–76.
4. Gibbons RJ, Verani MS, Behrenbeck T, et al. Feasibility of tomographic Tc-99m-hexakis-2-methoxy-2-methylpropyl-isonitrile imaging for the assessment of myocardial area at risk and the effect of acute treatment in myocardial infarction. *Circulation*. 1989;80:1277–1286.
5. Furutani Y, Shiigi T, Nakamura Y, et al. Quantification of area at risk in acute myocardial infarction by tomographic imaging. *J Nucl Med*. 1997;38:1875–1882.

6. Ceriani L, Verna E, Giovannella L, et al. Assessment of myocardium at risk by technetium-99m sestamibi during coronary artery occlusion: comparison between three tomographic methods of quantification. *Eur J Nucl Med.* 1996;23:31-39.
7. O'Connor MK, Gibbons RJ, Juni JE, O'Keefe J, Ali A. Quantitative myocardial SPECT for infarct sizing: feasibility of a multi-center trial evaluated using a cardiac phantom. *J Nucl Med.* 1995;36:1130-1136.
8. Chareonthaitawee P, Christian TF, O'Connor MK, et al. Noninvasive prediction of residual blood flow within the risk area during acute myocardial infarction: a multi-center validation study of patients undergoing direct coronary angiography. *Am Heart J.* 1997;134:639-646.
9. Christian TF, O'Connor MK, Schwartz RS, Gibbons RJ, Ritman EL. Technetium-99m MIBI to assess coronary collateral flow during acute myocardial infarction in two closed-chest animal models. *J Nucl Med.* 1997;38:1840-1846.
10. Pokropek TA, Craddock TD, Deconinck F. A file format for the exchange of nuclear medicine image data: a specification of Interfile version 3.3. *Nucl Med Commun.* 1992;13:673-699.
11. Christian TF, Schwartz RS, Gibbons RJ. Determinants of infarct size in reperfusion therapy for acute myocardial infarction. *Circulation.* 1992;86:81-90.
12. American College of Nuclear Physicians. Nuclear medicine imaging proficiency testing program simulator critique: 1996 IM—a myocardial perfusion study. Washington, DC: American College of Nuclear Physicians; 1996.
13. Tamaki N, Mukai T, Ishii Y, et al. Comparative study of thallium emission myocardial tomography with 180° and 360° data collection. *J Nucl Med.* 1982;23:661-666.
14. Coleman RE, Jaszczak RJ, Cobb FR. Comparison of 180° and 360° data collection in thallium-201 imaging using single-photon emission computed tomography (SPECT). *J Nucl Med.* 1982;23:655-660.
15. Go RT, MacIntyre WJ, Houser TS, et al. Clinical evaluation of 360° and 180° data sampling techniques for transaxial SPECT thallium-201 myocardial perfusion imaging. *J Nucl Med.* 1985;26:695-706.
16. Eisner RL, Nowak DJ, Pettigrew R, Fajman W. Fundamentals of 180° acquisition and reconstruction in SPECT imaging. *J Nucl Med.* 1986;27:1717-1728.
17. Knesaurek K, King MA, Glick SJ, Penney BC. Investigation of causes of geometric distortion in 180° and 360° angular sampling in SPECT. *J Nucl Med.* 1989;30:1666-1675.
18. Hoffman EJ. 180° compared with 360° sampling in SPECT [editorial]. *J Nucl Med.* 1982;23:745-747.
19. Maublant JC, Peycelon P, Kwaikowski F, et al. Comparison between 180° and 360° data collection in technetium-99m MIBI SPECT of the myocardium. *J Nucl Med.* 1989;30:295-300.
20. Folks R, Van Train K, Wong C, et al. Evaluation of Tc-MIBI SPECT acquisition parameters: circular vs. elliptical and 180° vs. 360° orbits [abstract]. *J Nucl Med.* 1989;30:795P-796P.
21. Hung JC, Mahoney DW, Johnston DL, Gibbons RJ. An optimal dual-size vial system for the cost-effective usage of Adenoscan. *J Nucl Cardiol.* 1998;5:161-166.
22. Nuyts J, Dupont P, Van der Maegdenbergh V, Vleugels S, Suetens P, Mortelmans L. A study of the liver-heart artifact in emission tomography. *J Nucl Med.* 1995;36:133-139.
23. LaCroix KJ, Tsui BMW, Hasagawa BH. A comparison of 180° and 360° acquisition for attenuation-compensated thallium-201 SPECT images. *J Nucl Med.* 1998;39:562-574.
24. O'Connor MK, Bothun E, Gibbons RJ. Influence of patient height and weight and type of stress on myocardial count density during SPECT imaging with thallium-201 and technetium 99m-sestamibi. *J Nucl Cardiol.* 1998;5:304-312.